

ON THE TIDAL RADIUS OF SATELLITES ON PROGRADE AND RETROGRADE ORBITS

GRZEGORZ GAJDA AND EWA L. LOKAS

Nicolaus Copernicus Astronomical Center, Bartycka 18, 00-716 Warsaw, Poland

Submitted to ApJ

ABSTRACT

A tidal radius is a distance from a satellite orbiting in a host potential beyond which its material is stripped by the tidal force. We derive a revised expression for the tidal radius of a rotating satellite which properly takes into account the possibility of prograde and retrograde orbits of stars. Besides the eccentricity of the satellite orbit, the tidal radius depends also on the ratio of the satellite internal angular velocity to the orbital angular velocity. We compare our formula to the results of two N -body simulations of dwarf galaxies orbiting a Milky Way-like host on a prograde and retrograde orbit. The tidal radius for the retrograde case is larger than for the prograde. We introduce a kinematic radius separating stars still orbiting the dwarf galaxy from those already stripped and following the potential of the host galaxy. We find that the tidal radius matches very well the kinematic radius.

Subject headings: galaxies: dwarf — galaxies: interactions — galaxies: kinematics and dynamics — galaxies: structure

1. INTRODUCTION

The tidal radius r_t is a theoretical boundary of a satellite object (e.g. a star cluster, a galaxy) beyond which its material is stripped by the tidal forces originating from the potential of a larger host object (e.g. another galaxy, a galaxy cluster). It was proposed for the first time by von Hoerner (1957) in the context of globular clusters orbiting around the Milky Way. A strict theoretical definition exists only for satellites on circular orbits, for which the tidal radius is identical to the position of L1/L2 Lagrange points (see Binney & Tremaine 2008). King (1962) argued that for an eccentric orbit of a satellite, a star located at the instantaneous tidal radius is stationary in a rotating reference frame and is attracted neither towards the satellite nor towards the host. He also argued that the satellites are truncated during pericenter passages to the size indicated by the pericentric tidal radius.

However, already Hénon (1970) and Keenan & Innanen (1975) noticed that retrograde orbits in the restricted three-body problem are stable up to much larger distances than prograde ones, exceeding the King (1962) tidal radius. Read et al. (2006) derived an expression for r_t that takes into account three basic types of orbits: prograde, radial and retrograde. Indeed, the tidal radius for retrograde orbits turned out to be larger than for radial ones, which in turn was larger than for prograde orbits.

Interactions of galaxies with the potential of larger objects have proved capable of transforming their morphology and kinematics on various scales: those of dwarf galaxies orbiting the Milky Way-like galaxy (Mayer et al. 2001; Kazantzidis et al. 2011), galaxies in groups (Villalobos et al. 2012) and clusters (Mastropietro et al. 2005; Bialas et al. 2015). One of the factors influencing the final outcome of such a process is the initial inclination of the galaxy disk with respect to its orbit (Villalobos et al. 2012; Lokas et al. 2015). The result of an encounter of equal-mass disk galaxies also depends on the direction of their rotation (Holmberg 1941;

Toomre & Toomre 1972).

The tidal radius is important for studying globular clusters (Webb et al. 2013) and dwarf galaxies (Lokas et al. 2013) as it can help disentangle their bound parts from the material which has been already lost and forms tidal tails (Küpper et al. 2010, 2012). Semi-analytical models of galaxy formation also rely on comparisons of the tidal radius to the size of the galaxy to describe timescales of stripping (Henriques & Thomas 2010; Chang et al. 2013).

In this paper we derive a new expression for the tidal radius, which properly takes into account both the eccentric orbit of the satellite and the orientation of its internal rotation. We apply this formula to N -body simulations of a disk dwarf galaxy orbiting a Milky Way-like host and compare its predictions to features detected in mass and velocity distributions of the dwarf.

2. DERIVATION

Let a dwarf galaxy with a spherically symmetric mass distribution $m(x)$ orbit around a host galaxy with a spherically symmetric mass distribution $M(x)$. In a reference frame centered on the dwarf the acceleration of a star belonging to the dwarf, located at \mathbf{x}_s , is given by

$$\ddot{\mathbf{x}}_s = -Gm(|\mathbf{x}_s|)\frac{\mathbf{x}_s}{|\mathbf{x}_s|^3} - GM(|\mathbf{x}_s - \mathbf{x}_h|)\frac{\mathbf{x}_s - \mathbf{x}_h}{|\mathbf{x}_s - \mathbf{x}_h|^3} - GM(|\mathbf{x}_h|)\frac{\mathbf{x}_h}{|\mathbf{x}_h|^3}, \quad (1)$$

where \mathbf{x}_h is the position of the host and G is the gravitational constant. The first term is the gravitational attraction by the dwarf galaxy, the second one is the attraction by the host galaxy and the last one is the inertial force arising because the reference frame is not inertial, as the dwarf is falling onto the host. The second term

can be expanded in the series for $|\mathbf{x}_s|/|\mathbf{x}_h| \ll 1$, yielding

$$\begin{aligned} \ddot{\mathbf{x}}_s = & -Gm(|\mathbf{x}_s|) \frac{\mathbf{x}_s}{|\mathbf{x}_s|^3} - GM(|\mathbf{x}_h|) \frac{\mathbf{x}_s}{|\mathbf{x}_h|^3} \\ & + GM(|\mathbf{x}_h|)[3 - p(|\mathbf{x}_h|)] \frac{(\mathbf{x}_s \cdot \mathbf{x}_h)\mathbf{x}_h}{|\mathbf{x}_h|^5} + \mathcal{O}[(|\mathbf{x}_s|/|\mathbf{x}_h|)^2], \end{aligned} \quad (2)$$

where $p(|\mathbf{x}_h|) = d \log M / d \log x|_{x=|\mathbf{x}_h|}$ is the logarithmic derivative of $M(x)$ calculated at $x = |\mathbf{x}_h|$ and the dot denotes the scalar product.

The second and third terms together are commonly referred to as the tidal force. It squeezes the dwarf in the plane perpendicular to the direction to the host and elongates it in the direction towards and away from the host. In such an environment an initially disk dwarf is likely to form a tidally induced bar (e.g. Lokas et al. 2014).

Let us change the reference frame to one rotating with a variable angular velocity $\boldsymbol{\Omega}$. New terms, the inertial forces, appear: the Euler force, the Coriolis force and the centrifugal force. The acceleration of the star now reads

$$\begin{aligned} \ddot{\mathbf{x}}_s = & -Gm(|\mathbf{x}_s|) \frac{\mathbf{x}_s}{|\mathbf{x}_s|^3} - GM(|\mathbf{x}_h|) \frac{\mathbf{x}_s}{|\mathbf{x}_h|^3} \\ & + GM(|\mathbf{x}_h|)[3 - p(|\mathbf{x}_h|)] \frac{(\mathbf{x}_s \cdot \mathbf{x}_h)\mathbf{x}_h}{|\mathbf{x}_h|^5} - \dot{\boldsymbol{\Omega}} \times \mathbf{x}_s \\ & - 2\boldsymbol{\Omega} \times \dot{\mathbf{x}}_s - \boldsymbol{\Omega} \times (\boldsymbol{\Omega} \times \mathbf{x}_s) + \mathcal{O}[(|\mathbf{x}_s|/|\mathbf{x}_h|)^2], \end{aligned} \quad (3)$$

where the cross denotes the vector product.

In order to proceed we need to make an assumption about the velocity of the star. Let us assume the star follows a circular orbit around the dwarf with angular velocity $\boldsymbol{\Omega}_s$, so its velocity in a non-rotating reference frame is $\boldsymbol{\Omega}_s \times \mathbf{x}_s$. In the rotating frame we have to subtract the velocity of the frame itself, therefore

$$\dot{\mathbf{x}}_s = (\boldsymbol{\Omega}_s - \boldsymbol{\Omega}) \times \mathbf{x}_s. \quad (4)$$

This equation describes the velocity of the star with respect to the dwarf galaxy, thus it should correspond to equation (3) in Read et al. (2006). However, they neglected the component due to the rotation of the reference frame. For example, if in the non-rotating frame the star was at rest with respect to the dwarf (so $\boldsymbol{\Omega}_s = 0$), in the rotating one there would still be a net relative velocity due to different velocities of the frame at the position of the star and at the center of the dwarf. This omission led to an incorrect interpretation, as we show below.

After substitution we obtain

$$\begin{aligned} \ddot{\mathbf{x}}_s = & -Gm(|\mathbf{x}_s|) \frac{\mathbf{x}_s}{|\mathbf{x}_s|^3} - GM(|\mathbf{x}_h|) \frac{\mathbf{x}_s}{|\mathbf{x}_h|^3} \\ & + GM(|\mathbf{x}_h|)[3 - p(|\mathbf{x}_h|)] \frac{(\mathbf{x}_s \cdot \mathbf{x}_h)\mathbf{x}_h}{|\mathbf{x}_h|^5} - \dot{\boldsymbol{\Omega}} \times \mathbf{x}_s \\ & - 2\boldsymbol{\Omega} \times (\boldsymbol{\Omega}_s \times \mathbf{x}_s) + \boldsymbol{\Omega} \times (\boldsymbol{\Omega} \times \mathbf{x}_s) + \mathcal{O}[(|\mathbf{x}_s|/|\mathbf{x}_h|)^2], \end{aligned} \quad (5)$$

which is the final formula for the acceleration of the star on a circular orbit around the dwarf galaxy, calculated in the frame rotating with a variable angular velocity. We note that up to this point vectors $\boldsymbol{\Omega}_s$ and $\boldsymbol{\Omega}$ are arbitrary.

We now derive the tidal radius for stars whose orbits lie in the same plane as the orbit of the dwarf. We choose $\boldsymbol{\Omega}$ so that the unit vector $\hat{\mathbf{x}}_h = \mathbf{x}_h/|\mathbf{x}_h|$, pointing from the dwarf towards the host, is constant in time. In such a setup $\boldsymbol{\Omega} \parallel \boldsymbol{\Omega}_s$ and $\boldsymbol{\Omega} \perp \mathbf{x}_s$. Using these properties we can rewrite double vector products obtaining

$$\begin{aligned} \ddot{\mathbf{x}}_s = & -Gm(|\mathbf{x}_s|) \frac{\mathbf{x}_s}{|\mathbf{x}_s|^3} - GM(|\mathbf{x}_h|) \frac{\mathbf{x}_s}{|\mathbf{x}_h|^3} \\ & + GM(|\mathbf{x}_h|)[3 - p(|\mathbf{x}_h|)] \frac{(\mathbf{x}_s \cdot \mathbf{x}_h)\mathbf{x}_h}{|\mathbf{x}_h|^5} - \dot{\boldsymbol{\Omega}} \times \mathbf{x}_s \\ & + 2(\boldsymbol{\Omega} \cdot \boldsymbol{\Omega}_s)\mathbf{x}_s - |\boldsymbol{\Omega}|^2 \mathbf{x}_s + \mathcal{O}[(|\mathbf{x}_s|/|\mathbf{x}_h|)^2]. \end{aligned} \quad (6)$$

Stars are mainly stripped when they are at the smallest or largest distance from the host and leave the vicinity of the dwarf through the L1 and L2 Lagrange points. To find the component of the acceleration along the direction towards the host assuming $\mathbf{x}_s \parallel \mathbf{x}_h$ we multiply the above equation by $\hat{\mathbf{x}}_s = \mathbf{x}_s/|\mathbf{x}_s|$ to get

$$\begin{aligned} \ddot{\mathbf{x}}_s \cdot \hat{\mathbf{x}}_s = & -Gm(x_s) \frac{1}{x_s^2} + GM(x_h)[2 - p(x_h)] \frac{x_s}{x_h^3} \\ & + \Omega^2 \left(2 \frac{\Omega_s}{\Omega} - 1 \right) x_s + \mathcal{O}[(x_s/x_h)^2], \end{aligned} \quad (7)$$

where we denoted magnitudes of each vector as $|\mathbf{a}| = a$, except for Ω_s which obeys relation $\boldsymbol{\Omega} \cdot \boldsymbol{\Omega}_s = \Omega\Omega_s$, i.e. its sign depends on its direction with respect to the direction of $\boldsymbol{\Omega}$.

We can parametrize the orbital angular velocity as $\Omega^2 = [GM(x_h)]/[x_h^3 \lambda(x_h)]$. The parameter $\lambda(x_h)$ depends on the orbit of the dwarf and details of the host potential. For a circular orbit $\lambda = 1$, for a point-mass host $\lambda(x_h) = x_h/[a(1 - e^2)]$, where a is the major semi-axis and e is the eccentricity. One may wonder if we can assume something about Ω_s , for example that it is equal to the circular velocity in the dwarf, i.e. $\Omega_s = [Gm(x_s)/x_s^3]^{1/2}$. However, such an assumption leads to incorrect results, as we demonstrate below.

The tidal radius r_t is commonly defined as the distance from the center of the dwarf where there is neither acceleration towards the dwarf nor towards the host (e.g. King 1962; Read et al. 2006). In our case this can be written as $\ddot{\mathbf{x}}_s \cdot \hat{\mathbf{x}}_s|_{x_s=r_t} = 0$. After applying this relation, substituting for Ω^2 and truncating the series we obtain the equation for r_t

$$r_t = x_h \left(\frac{[m(r_t)/M(x_h)]\lambda(x_h)}{2\Omega_s/\Omega - 1 + [2 - p(x_h)]\lambda(x_h)} \right)^{1/3}, \quad (8)$$

$$2\Omega_s/\Omega > -[2 - p(x_h)]\lambda(x_h) + 1. \quad (9)$$

The above inequality has to be fulfilled, otherwise the tidal radius does not exist. In such a situation the acceleration points towards the dwarf. One can interpret this as the tidal radius being infinite. However, we assumed that $r_t \ll x_h$, hence such an extrapolation is not valid.

If we assume the simplest setup, namely a point-mass host and dwarf (so $p = 0$) and a circular orbit of the

dwarf ($\lambda = 1$), we obtain

$$r_t = x_h \left(\frac{1}{2\Omega_s/\Omega + 1} \frac{m}{M} \right)^{1/3}, \quad (10)$$

$$\Omega_s/\Omega > -1/2. \quad (11)$$

Assuming further that $\Omega_s/\Omega = 1$ we recover the expression for the L1/L2 Lagrange points. This is straightforward to understand: a star located in the L1/L2 point is stationary in the rotating reference frame, hence it rotates around the dwarf with the same angular velocity as the dwarf revolves around the host. This shows the misleading physical reasoning of Read et al. (2006): in their framework the Lagrange points were recovered for the stars on *radial* orbits. However, that was a coincidence because for their radial orbits they obtained the force equation corresponding to the *prograde* case. This also explains why Lokas et al. (2013) obtained good match of the tidal radius to N -body simulations assuming radial orbits of the stars, whereas the dwarfs were in fact on a mildly prograde orbit.

From the above it is also clear why we cannot assume the star to be moving with angular velocity $\Omega_s = [Gm(x_s)/x_s^3]^{1/2}$. In such case the angular velocity at the true distance of the L1/L2 points would be $\Omega_s = \sqrt{3}\Omega$, thus significantly overestimated. Consequently, the tidal radius would be underestimated. Therefore, as Ω_s one has to use the angular velocity *already perturbed* by the host.

It may seem that for a dwarf on a retrograde orbit ($\Omega_s < 0$), which spins sufficiently fast, the tidal radius is infinite. However, as we have already argued, in this case our approximation breaks down. Moreover, in real objects $|\Omega_s|$ decreases with the distance from the center, therefore there will exist a radius where the necessary inequality will be fulfilled.

If we assume in equation (8) that the star is at the (instantaneous) Lagrange point ($\Omega_s/\Omega = 1$) we can recover two known expressions for the tidal radius. For the dwarf on a circular orbit around an extended host we recover the formula 8.108 from Binney & Tremaine (2008). For an elliptical orbit around a point-mass host we recover the limiting radius formula from King (1962). We emphasize that this exceptionally simple formula $r_t = x_{h,peri} \{m/[M(3+e)]\}^{1/3}$ is valid only at the pericenter of the satellite's orbit.

3. COMPARISON TO N -BODY SIMULATIONS

Any formula should be compared to a realistic situation in order to check its validity and the assumptions made during the derivation. We shall use two of the N -body simulations studied in detail by Lokas et al. (2015) that followed the evolution of a dwarf galaxy around a Milky Way-like host. The live realization of a Milky Way-like galaxy consisted of an NFW (Navarro et al. 1995) dark matter halo with a virial mass of $7.7 \times 10^{11} M_\odot$ and concentration $c = 27$ and an exponential disk of mass $3.4 \times 10^{10} M_\odot$ with a radial scale length 2.88 kpc and thickness 0.44 kpc. The dwarf galaxy had an NFW halo of $10^9 M_\odot$ and $c = 20$ and a disk of mass $2 \times 10^7 M_\odot$, the radial scale length 0.41 kpc and thickness 0.082 kpc. Each component of each galaxy contained 10^6 particles.

The dwarf galaxy was initially placed at an apocenter

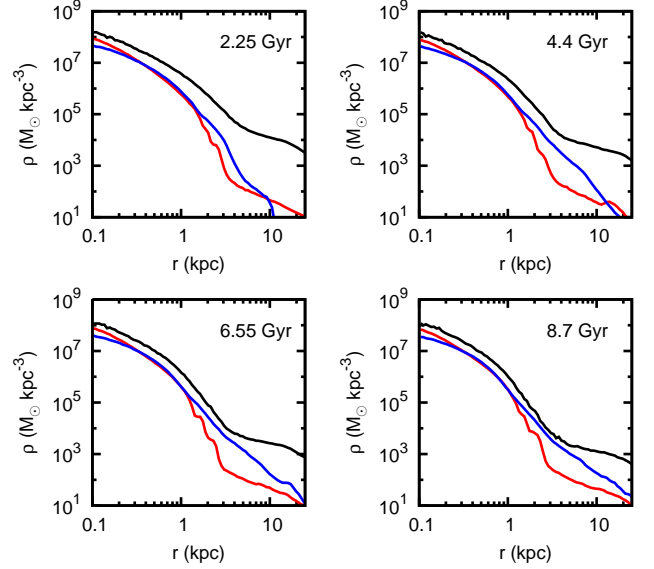


FIG. 1.— Density profiles of the stellar component of the dwarf galaxy for the prograde model (red) and the retrograde model (blue), as well as dark matter density profile (black) at consecutive apocenters.

of an eccentric orbit around the host galaxy with apocenter and pericenter distances of 120 and 25 kpc, respectively. The plane of the orbit was the same as the plane of the host's disk. The only parameter which was varied between the simulations was the initial inclination of the disk of the dwarf with respect to the orbit. Here we will use only two configurations: the exactly prograde and the exactly retrograde, which in Lokas et al. (2015) were referred to as I0 and I180, respectively.

In principle, the tidal radius formula (8) applies to individual particles in the dwarf, as each star has a different angular velocity Ω_s . In order to apply it to the dwarf as a whole, we measured the $\Omega_s(x_s)$ profile, i.e. the profile of the mean angular velocity component parallel to the orbital angular velocity of the dwarf. Obviously, particles in the dwarf are not on exactly circular orbits and have non-negligible radial velocities. As a result, an additional component of the Coriolis force appears. However, it is orthogonal to \mathbf{x}_s and, consequently, does not have any impact on the force component along \mathbf{x}_s .

The right-hand side of equation (8) depends on r_t , thus it is an implicit formula for the tidal radius, which can be solved numerically. In order to obey the assumptions, from now on we will treat the disk of the host as a point mass. Furthermore, we calculated $m(r_t)$ assuming spherical symmetry of the dwarf galaxy mass distribution. While these approximations introduce some error, we consider it negligible, as it only underestimates the gravitational force of the disks of both galaxies, which are at least an order of magnitude less massive than their dark matter haloes. The calculation of $\lambda(x_h)$ was carried out assuming that the dwarf is a point mass object orbiting a spherical host.

In Figure 1 we show density profiles of the stellar component during consecutive apocenters for both models. In addition, we plot the profile of the dark matter component, which was the same in both cases. In the density profiles of the prograde model there is a clear break where the main body of the dwarf ends and the tidal tails begin.

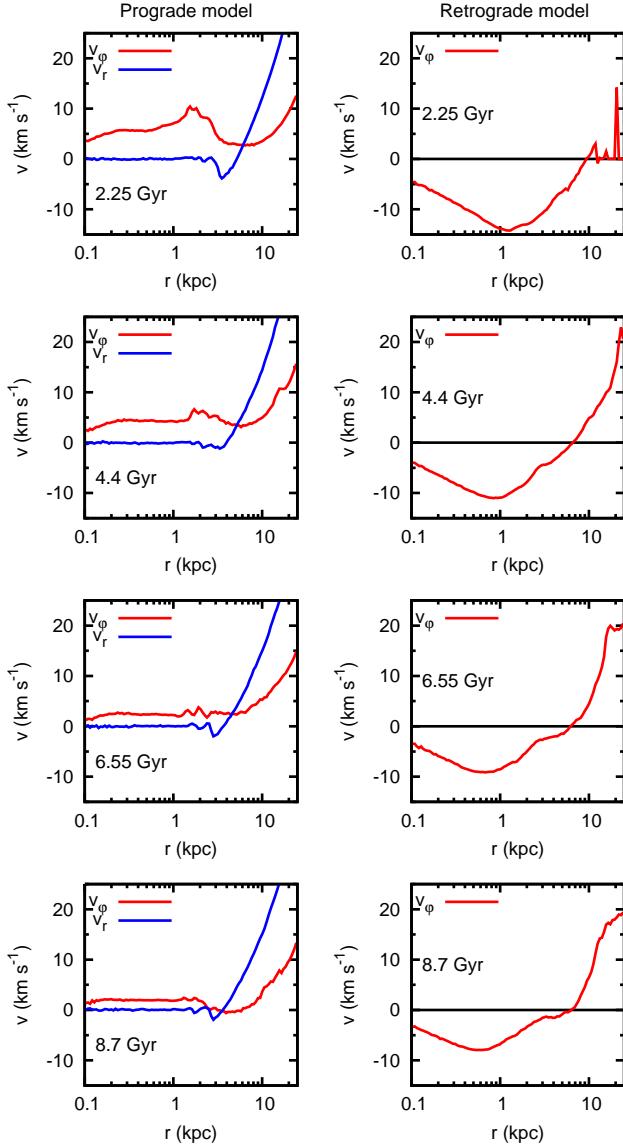


FIG. 2.— *Left column:* The rotational velocity (red) and the radial velocity (blue) of the dwarf on the prograde orbit. *Right column:* The rotational velocity of the dwarf on the retrograde orbit. Negative values indicate that the dwarf counter rotates with respect to its orbit. Rows of panels correspond to consecutive apocenters.

On the other hand, the profiles in the retrograde model are rather featureless and close to a power law.

For their mildly prograde models, Lokas et al. (2013) compared the break radius r_b to the theoretical tidal radius. Here, we were only able to locate the break in the prograde model and to measure it we used the method of Johnston et al. (2002). At each radius we calculated slopes of the density profile interior and exterior to that radius. Comparing the two slopes we searched for the innermost difference larger than the assumed threshold.

Stripping of the stars should also influence their kinematics. This is because in the first approximation the stars bound to the dwarf are mostly influenced by the dwarf potential, whereas the motion of the stripped ones is governed by the potential of the host. Therefore, we introduce the *kinematic radius* r_k beyond which the kinematics of the particles is no longer dominated by the

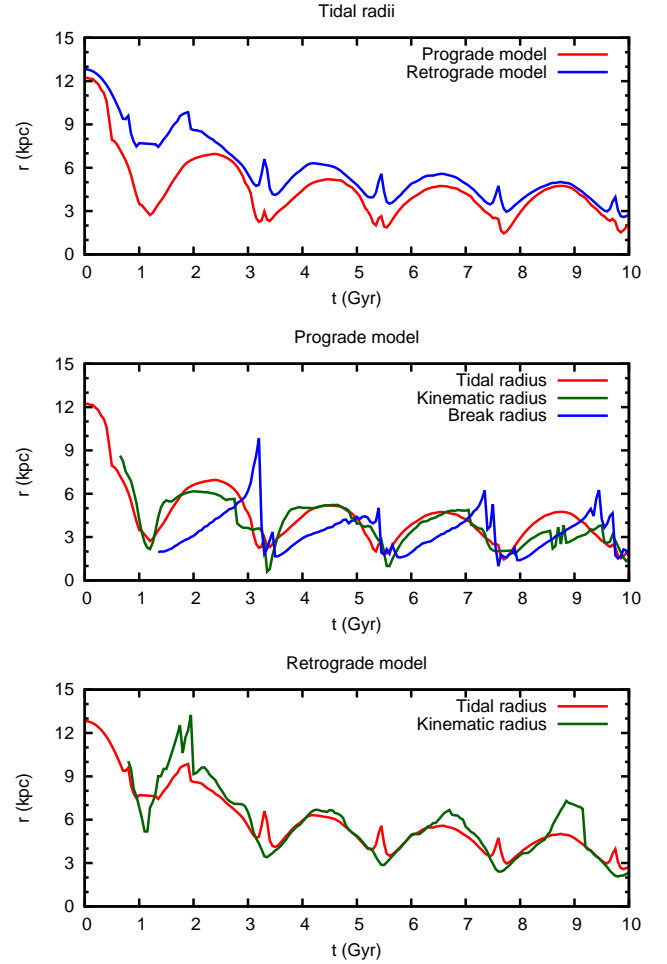


FIG. 3.— *Top:* Tidal radii calculated for the prograde (red) and the retrograde (blue) model. *Middle:* Tidal radius (red), kinematic radius (green) and break radius (blue) for the prograde model. *Bottom:* Tidal radius (red) and kinematic radius (green) for the retrograde model.

potential of the dwarf.

Particular realizations of this definition are different in both models. To illustrate this, in Figure 2 we plot profiles of the rotational velocity $v_\phi = r\Omega_s$ of the dwarfs at the consecutive apocenters. The inner parts of the retrograde model counter-rotate with respect to the orbital angular velocity, as indicated by the negative values of v_ϕ . The maximum of the velocity curve slowly decreases at subsequent apocenters due to mass loss. Particles which were stripped and are already far away (more than 10 kpc) have positive angular velocity with respect to the center of the dwarf, as they orbit the host. Taking this into account, we define the kinematic radius as the one where $\Omega_s = 0$.

In the case of the prograde model, the angular velocity in the inner parts decreases significantly as the dwarf is transformed and the random motions start to dominate (see e.g. Fig. 2 in Lokas et al. 2015). In the outer parts, v_ϕ grows similarly as in the retrograde model. Unfortunately, there is no such a striking feature as in the retrograde case. One can see a minimum in the outer parts, but it is very wide and shallow, if present at all, therefore it is not a suitable proxy for the kinematic radius. Instead, we define r_k as a radius where the radial

velocity is equal to the rotational velocity, i.e. $v_r = v_\varphi$. We note that there is a region in the profiles of v_r where $v_r < 0$, indicating that some particles are reaccreted onto the dwarf.

In Figure 3 we show tidal radii calculated from formula (8) and compare them with the kinematic and break radii obtained from N -body simulations for the prograde and retrograde model. The tidal radius for the retrograde model is always larger than for the prograde model. However, the difference is smaller later on because the rotation of the prograde dwarf slows down with time. Small peaks in r_t measurements around the pericenters are caused by the Coriolis force originating from the movement of the whole dwarf on such an elongated orbit that locally exceeds the tidal force. This behavior might be different if we included higher order terms in the tidal force.

The kinematic radius agrees remarkably well with the tidal radius. However, the agreement is worse between the fourth and fifth pericenter. In the prograde case it is because the stellar component has already significantly evolved from the initial disk configuration. In the retrograde case, the profile of the angular velocity in the outer parts is very flat and it does not cross zero up to a large radius, possibly due to numerical errors. On the other hand, r_b is only a rough estimate of the tidal radius. As discussed by Lokas et al. (2013), it is because the density distribution needs time to respond to the external forces.

4. CONCLUSIONS

In this work we studied the tidal radius of satellites orbiting in a host potential. We derived an improved formula for r_t for stars revolving around the satellite in the same plane as the satellite orbits the host. Our formula (8) properly takes into account that the star might be on a prograde or retrograde orbit. We verified our formula against N -body simulations of a disk dwarf galaxy on a co-planar orbit around a Milky Way-like host. The tidal radius corresponds to the kinematic radius, i.e. the radius beyond which kinematics of the stellar particles is dominated by the host potential and the particles no longer orbit the dwarf galaxy.

Our derivation depends on two basic assumptions: the stars orbit the dwarf on circular orbits and they are

stripped in the vicinity of the line connecting the dwarf and the host (i.e. near L1/L2 Lagrange points). While the latter seems to be fulfilled based on the analysis of tidal tails (Klimontowski et al. 2009; Lokas et al. 2013), the former is quite disputable. For example, Szebehely (1967) showed that in the restricted three-body problem prograde orbits of the smallest body get complicated when particles approach the Lagrange points. On the other hand, retrograde orbits are fairly circular. Thus, we expect that our calculations are more robust in the retrograde case.

Using an improved impulse approximation, D’Onghia et al. (2009, 2010) proposed that stripping of the satellites is of resonant origin. Namely, for prograde encounters particles have largest velocity gains if their $\alpha = \Omega_s/\Omega \sim 1$ during the pericenter passage. Lokas et al. (2015) calculated radii at which $\alpha = 1$ for the prograde model. In the vicinity of the pericenter, where most of the stripping occurs, $r_{\alpha=1} < r_t$, i.e. resonant radius is smaller than the tidal radius.

In view of the above, we may interpret the mechanism of stripping in the case of coplanar encounters as follows. In the prograde case the material in the outer parts of the disk is accelerated and pushed away by the resonant mechanism. When it travels beyond the tidal radius it becomes unbound from the dwarf and starts to follow the potential of the host. Some of this material is reaccreted by the dwarf, as its tidal radius increases when the dwarf recedes from the pericenter. In the retrograde case stellar particles are accelerated much more weakly (see Fig. 4 of D’Onghia et al. 2010), so they are driven out of the dwarf, but they remain in its vicinity, as confirmed by their density profiles (Fig. 1).

Our analytic calculations are based on simplifying assumptions, which are not able to grasp other possible inclinations of the dwarf’s disk and the variety of particle orbits. More investigation is needed to establish a proper connection between the stability of individual particle orbits and the general behavior of the density distribution and stripping.

This work was supported by the Polish National Science Centre under grant 2013/10/A/ST9/00023. We acknowledge discussions with E. D’Onghia.

REFERENCES

- Bialas, D., Lisker, T., Olczak, C., et al. 2015, *A&A*, 576, A103
 Binney, J., & Tremaine, S. 2008, *Galactic Dynamics* (2nd ed.; Princeton, NJ: Princeton Univ. Press)
 Chang, J., Macciò, A. V., & Kang, X. 2013, *MNRAS*, 431, 3533
 D’Onghia, E., Besla, G., Cox, T. J., & Hernquist, L. 2009, *Nature*, 460, 605
 D’Onghia, E., Vogelsberger, M., Faucher-Giguere, C. A., & Hernquist, L. 2010, *ApJ*, 725, 353
 Henriques, B. M. B., & Thomas, P. A. 2010, *MNRAS*, 403, 768
 Holmberg, E. 1941, *ApJ*, 94, 385
 Hénon, M. 1970, *A&A*, 9, 24
 Johnston, K. V., Choi, P. I., & Guhathakurta, P. 2002, *AJ*, 124, 127
 Kazantzidis, S., Lokas, E. L., Callegari, S., et al. 2011, *ApJ*, 726, 98
 Keenan, D. W., & Innanen, K. A. 1975, *AJ*, 80, 290
 King, I. 1962, *AJ*, 67, 471
 Klimontowski, J., Lokas, E. L., Kazantzidis, S., et al. 2009, *MNRAS*, 400, 2162
 Küpper, A. H. W., Kroupa, P., Baumgardt, H., & Heggie, D. C. 2010, *MNRAS*, 407, 2241
 Küpper, A. H. W., Lane, R. R., & Heggie, D. C. 2012, *MNRAS*, 420, 2700
 Lokas, E. L., Athanassoula, E., Debattista, V. P., et al. 2014, *MNRAS*, 445, 1339
 Lokas, E. L., Gajda, G., & Kazantzidis, S. 2013, *MNRAS*, 433, 878
 Lokas, E. L., Senczuk, M., Gajda, G., & D’Onghia, E. 2015, *ApJ*, in press, arXiv:1505.00951
 Mastropietro, C., Moore, B., Mayer, L., et al. 2005, *MNRAS*, 364, 607
 Mayer, L., Governato, F., Colpi, M., et al. 2001, *ApJ*, 559, 754
 Navarro J. F., Frenk C. S., & White S. D. M. 1995, *MNRAS*, 275, 720
 Read, J. I., Wilkinson, M. I., Evans, N. W., et al. 2006, *MNRAS*, 366, 429
 Szebehely, V., *Theory of orbits. The restricted problem of three bodies*, 1967 (New York, NY: Academic Press)
 Toomre, A., & Toomre, J. 1972, *ApJ*, 178, 623

Villalobos, Á., De Lucia, G., Borgani, S., & Murante, G. 2012,
MNRAS, 424, 2401
von Hoerner, S. 1957, ApJ, 125, 451

Webb, J. J., Harris, W. E., Sils, A., & Hurley, J. R. 2013, ApJ,
764, 124